



Experiment to Investigate the Relationship Between the Third-Body Layer and the Occurrence of Squeals in Dry Sliding Contact

Narinder Singla¹ · Jean-François Brunel¹ · Alexandre Mège-Revil¹ · Haytam Kasem^{2,3} · Yannick Desplanques¹

Received: 15 July 2019 / Accepted: 31 October 2019 / Published online: 18 November 2019
© Springer Science+Business Media, LLC, part of Springer Nature 2019

Abstract

Braking is an energy dissipation mechanism used to restrict the movement of vehicles. Friction brakes may induce vibrations and noise. These effects constitute a major shortcoming related to the functioning of friction braking systems. Known as brake squeal, this phenomenon involves unstable vibrations induced by coupling modes between components in frictional contact leading to large amplitude vibrations. Despite significant progress in experimental techniques and numerical modeling, the origin of squeal occurrence remains misunderstood and is still a matter of debate. It is, however, commonly admitted that squeal is affected by many different factors on both micro and macro scales. In addition, a close correlation between wear and squeal occurrence in braking system has been reported. This study examines linking the change in the third-body layer with the occurrence of squeals in sliding dry contact. A simplified customized test rig was used with a transparent glass disc and an artificial alumina third-body. Results show that squeal occurrence is strongly linked to the densification and redistribution of the third-body, as well as internal flows in the interface.

Keywords Brake squeal · Friction-induced vibrations · Tribological circuit · Third-body flows

List of Symbols

Q_s (ext)	External third-body source flow
Q_s (int)	Internal third-body source flow
Q_e	Particles wear-out
Q_r	Third-body recirculation flow
Q_i	Internal third-body flow

1 Introduction

Braking is a vital function that helps to control vehicle motion and therefore ensures the safety of passengers. Among the different braking technologies used in transport (friction, eddy current, rheostatic, etc.), braking by friction (considered the most effective, particularly in cases of

emergency) is still the most commonly used. Although friction brakes have been improved considerably over the years, certain fundamental problems related to their use remain unresolved. The most frequent of these problems are cracking within brake discs due to thermal fatigue [1], friction instabilities [2], wear [3–5] and noise emissions among them squeal [6, 7]. Indeed, vibrations lead to a wide array of noises at various frequencies. Depending upon the involved frequencies and the nature of vibrations, noises can be classified as squeal, squeak, groan, chatter, judder, moan, hum, etc. [8]. Of these, brake squeal is the most troublesome for both people as well as the environment. Since squeal is a noise with a high frequency and acoustic pressure (above 1 kHz and 80 dB), it may be associated with high frequency and large amplitude vibrations under sliding conditions [9]. Despite recent significant progress in processing techniques, characterization tools, and computational algorithms, the fundamental understanding of physical conditions leading to squeal is still lacking, since it is inevitably affected by many different factors on both micro and macro scales.

Various mechanisms for the dynamic analysis for the occurrence of squeal have been proposed on the macro scale, i.e., negative friction coefficient sliding velocity slope, sprag-slip, flutter instabilities, stick-slip, mode lock-in [10, 11]. Although these mechanisms can be interrelated, the

✉ Jean-François Brunel
jean-francois.brunel@polytech-lille.fr

¹ Univ. Lille, CNRS, Centrale Lille, FRE 2016 – LaMcube – Laboratoire de mécanique multiphysique multiéchelle, 59000 Lille, France

² Department of Mechanical Engineering, Technion, 32000 Haifa, Israel

³ Department of Mechanical Engineering, Azrieli College of Engineering, 9103501 Jerusalem, Israel

instability is due to mode-coupling phenomenon. To predict the unstable modes, complex eigenvalues analysis of the brake system is popular as a numerical tool [7, 12]. In this spirit, Conglin et al. showed by experimental approach that frictional vibration and noise mostly occurred during the slip process of stick–slip mechanism [13]. Massi et al. studied experimentally the origin of squeal using a pin-on-disc test rig. They showed that the dynamic instabilities of tribosystem are the main cause for brake squeal [14]. Recently, Bonnay et al. published a numerical study on the effect of contact's geometric imperfections on the propensity for squealing. They concluded that 'disc thickness variation' as well as 'surface-layer distribution' have a strong influence on the dynamic behaviour and the mode lock-in, as well [15].

On meso and micro scales, the third-body approach suggested by Godet [16] and Berthier [17] implies that wear particle compaction plays a major role in the formation of such surface layers. Jacko et al. reported that when stable friction films, commonly called glaze, are readily formed for a given friction couple, a stable friction level and low wear rate can be maintained at various temperatures, as long as the friction film is kept undestroyed [18]. Other studies reveal that in the case of braking, the third-body present on the rubbed surfaces is composed of several components such as iron, iron oxides, copper oxide, copper sulphide, barium sulphate, carbonaceous products and several other phases [19]. Considering the internal disc/pad interface during friction, some studies have shown the formation of some flat contact plateaus on the composite pad, called primary plateaus, while wear debris, called secondary plateaus, are being accumulated and compacted around the primary plateaus [20]. In the same study the authors showed that when the contact situation changes during friction, the secondary contact plateaus disintegrate, and a progressive removal of this compacted debris occurs. The contact time–space evolution, the formation of well-established third-body layers, and the interactions between internal third-body flows have been illustrated in several studies [21, 22]. Recently, an experimental study along with numerical simulation of the sliding interface explained that the size of the contact plateau distribution affects the stick–slip amplitude and oscillation frequencies of brake friction materials [23]. In this context, the complexity of brake squeal comprehension resides in the fact that these squeals depend upon the changes in microscopic friction conditions as well as the macroscopic coefficient of friction, which themselves strongly depend upon disc surface topography [24]. Some studies reported the initiation of cracks at the pad contact surfaces as well as material exfoliations in the third-body when squeals occur [7]. In addition, many research works reported a close correlation between wear and squeal occurrence in braking system [25–27].

Despite recent significant improvements in experimental observation tools for sliding contact, many researchers

prefer adopting theoretical approaches, i.e. discrete element methods [28], cellular automata [29, 30], or movable cellular automata [31, 32]. These theoretical methods have been used to model tribofilm at the disc/pad interface as well as to describe surface topography. These published works allow the conclusion that contact is affected by the phenomena occurring at, on one hand the small scales related to space (microscopic contact effects) and time (high-frequency vibrations), and on the other hand, at large scales (wear, behaviour of the tribological triplet and dynamics of the whole brake system). As a consequence, it is clear that squeal is a complex problem involving strongly interdisciplinary issues, which requires an adequate approach that should combine both tribological and dynamic analyses [33].

“Classic” experimental studies, related to squeal issues in particular and tribology in general, imply worn surface observation post-friction [34]. The shortcoming of such observations resides in the fact that after opening the contact, much vital information related to the dynamic interface is definitively lost. If one has to understand the squeal, then it is important to be able to measure *in situ* the parameters involved and follow their time–space variation during the experiment. This is especially true if we consider the complex tribological circuit of the third-body in general proposed by Berthier [17] and particularly in braking system proposed by Desplanques [22, 35] as shown in Fig. 1a. It is admitted that the tribological circuit of third-body is able to continually change the friction surface and thus the load-bearing area. In addition, it is constantly affected by many factors such as (i) external sources (ii) internal sources of third-body, including adhesion and chemical reactions [4] (iii) ejection and reintroduction of third-body particles in the contact. In a recent study, it is also observed that a modification in the surrounding atmosphere of the sliding interface (from dry air to inert atmosphere of argon) leads to change in the tribological and vibrational behaviour as the inert atmosphere changes the nature of the third-body flows by restricting oxidation [36]. Considering all these factors to access information, it is clear that following the tribological circuit is a very complex task from an experimental point of view, particularly due to the inaccessibility of the contact during friction.

Therefore, a realistic approach needs to be simplified as much as possible while keeping the possibility to introduce somehow an artificial controlled third-body instead of undergoing uncontrolled natural wear particles coming from the first bodies (i.e., pad and disc). In addition, the approach should allow the *in situ* observation of the interface and to follow its time–space variation. The strategy is to develop a new experiment based on an elementary tribological circuit allowing to avoid the recirculation of third-body particles as shown in Fig. 1b. To achieve such an elementary tribological circuit, the materials (first and third-bodies) should

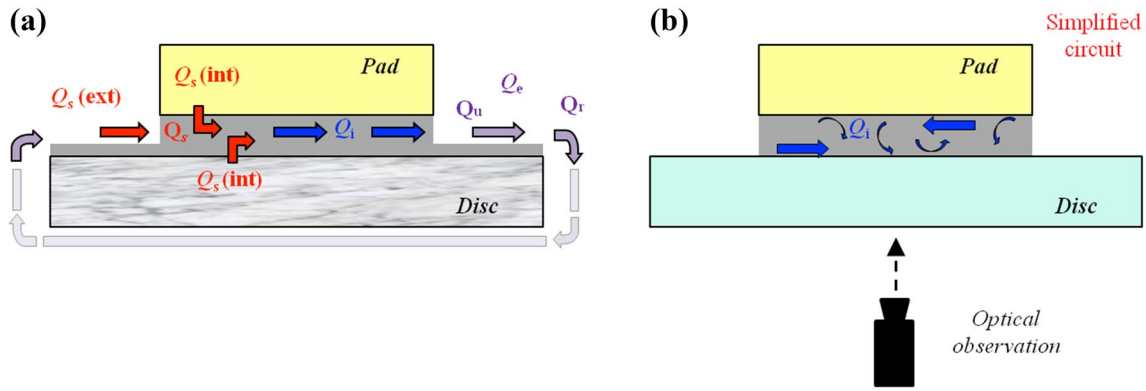


Fig. 1 **a** Tribological circuit and related third-body flows according to Berthier [15]; **b** Reduced tribological circuit to internal third-body flows

be chosen in such a way to reduce, as much as possible, physical coupling at the interface, for instance, in case of interfacial chemical reactions. In addition, the operational parameters of the experiment have to be chosen so that the wear of first bodies has negligible effects on the tribological circuit and remains sufficiently low to maintain adequate visibility of the contact area when using a transparent disc for optical monitoring during friction.

In the light of the above, the objective of the present study is to investigate experimentally the behaviour of the granular third-body layer in bearing and how it evolves during friction from silent to noisy situations. For this reason, a cohesive layer of an artificial third-body (alumina particles chemically inert) was chosen to achieve a thick layer instead of natural wear particles. To do so, an elementary experimental test rig allowing for the instrumentation of operational conditions leading to the occurrence of squeal during friction tests was used. The test rig was adjusted to work with limited natural vibrational modes and frequencies susceptible

to mode-coupling necessary for an understanding of the physical phenomena involved. Finally, a transparent glass disc was used to allow the *in situ* optical observation of the contact area. This article introduces the description of the experimental approach, the experimental set-up, and the material used (first and third-bodies). Finally, it discusses some experiments.

2 Experimental Set-Up and Materials

2.1 Experimental Set-Up and Instrumentation

Friction tests were performed on a customized test rig built on the basis of a pin-on-disc configuration and having an elementary architecture regarding vibrations. Figure 2 gives a general view and a schematic of the test rig that is extensively described in the reference. The set-up was designed

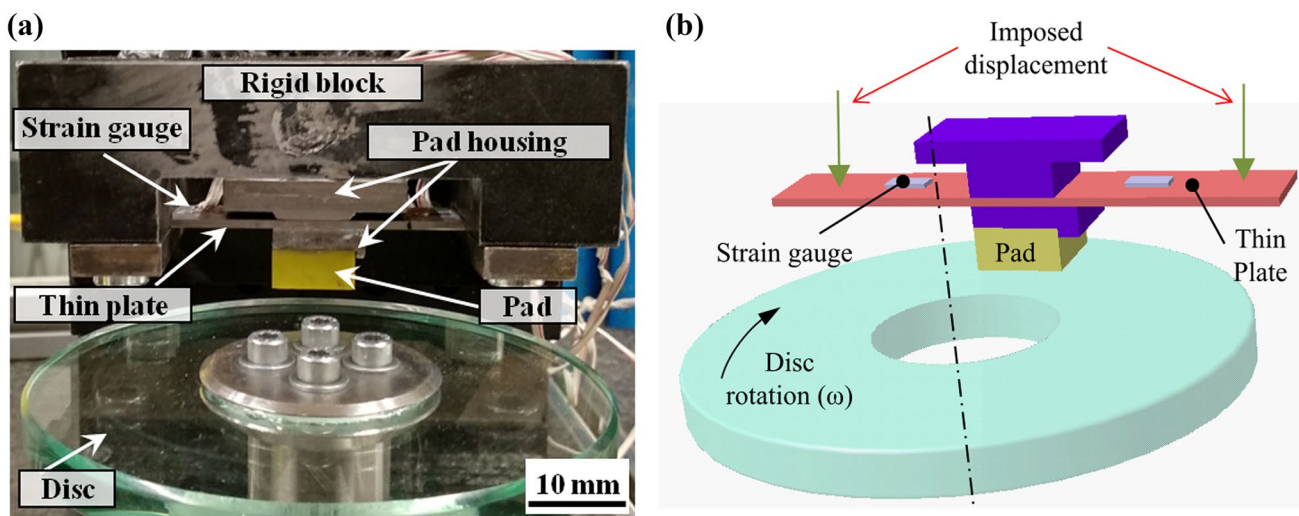


Fig. 2 Experimental set-up: **a** general view and **b** schematic

to study sliding contact-induced vibrations in a well-known dynamical environment [15, 33, 37].

The number of parts was intentionally reduced to minimize joints between parts of the system. This pin-on-disc set-up contains a flexible elastic thin plate made of steel, on which the pad (friction material) is affixed at its center by means of pad housing. A controlled displacement applied to the two extremities of the thin plate pushes down the pad and brings it into contact with the rotating disc; the normal loading of the contact is obtained due to the bending of the thin plate as illustrated in Fig. 2b.

It is important to note that the loading is sensitive to the displacement of the pad as well as the flatness deviation of the friction surfaces of both the pad and the disc. It is also in a disc brake. Therefore, strain gauges were glued to the thin plate to measure its elastic strain. Strain measurements allow computing accurately the applied normal load by means of a calibration factor initially determined. The calibration procedure shows a linear behaviour and a low sensitivity of the applied load to the location of the contact in the apparent contact area. During the tests the resulting normal load and the sound pressure measured by a microphone located close to the contact were recorded at high frequency using a Graphtec acquisition system.

In addition, the variation of the load-bearing contact was observed by an optical camera (Nikon D7100 with a lens 105 mm), and the acquisition frequency was set at 60 frames per second. The camera recorded the contact interface through the bottom part of the transparent glass disc. To do so, a mirror inclined at 45 degrees was placed below the disc as shown in Fig. 3. To improve the quality of the images recorded by the optical camera during the tests, an

external source of incident light was used as well. All tests were performed at room temperature of 20–22 °C, the relative humidity ranging between 35 and 40%.

2.2 Materials

In this study, the tested friction pair was composed of a glass disc and a pad made of compressed polyurethane resin. The use of optical transparent glass disc enables it to observe the contact interface through the disc. The glass disc with an inner diameter 40 mm, outer diameter 120 mm, and thickness 10 mm, was mounted on the tribometer as shown in Fig. 2. The friction surface of the pad is of 20 × 20 mm with 10 mm thickness. The artificial third-body consists of alumina powder, with particle size of 100–150 nm. The choice of the particle size, considerably larger than the nanometer size of the natural third-body particles involved in braking [3], helps to obtain a sufficiently thick layer of third-body able to accommodate the “flat” pad-disc contact without involving natural wear (negligible) of first bodies. More precisely, a large thickness of the third-body layer provides the tribosystem with the necessary degrees of freedom to accommodate pad-disc flatness and alignment deviations that evolve during friction following the disc undulation. Moreover, the large alumina-particle size leads to the formation of third-body plateaus sufficiently large to be observed using an optical camera. In addition, the yellow color of the pad and the white color of the alumina powder facilitate the optical observation of the contact interface and make it possible to follow its time–space variation. The size of the used alumina particles (100–150 nm) is sufficiently small to obtain good cohesion within the granular system, making it

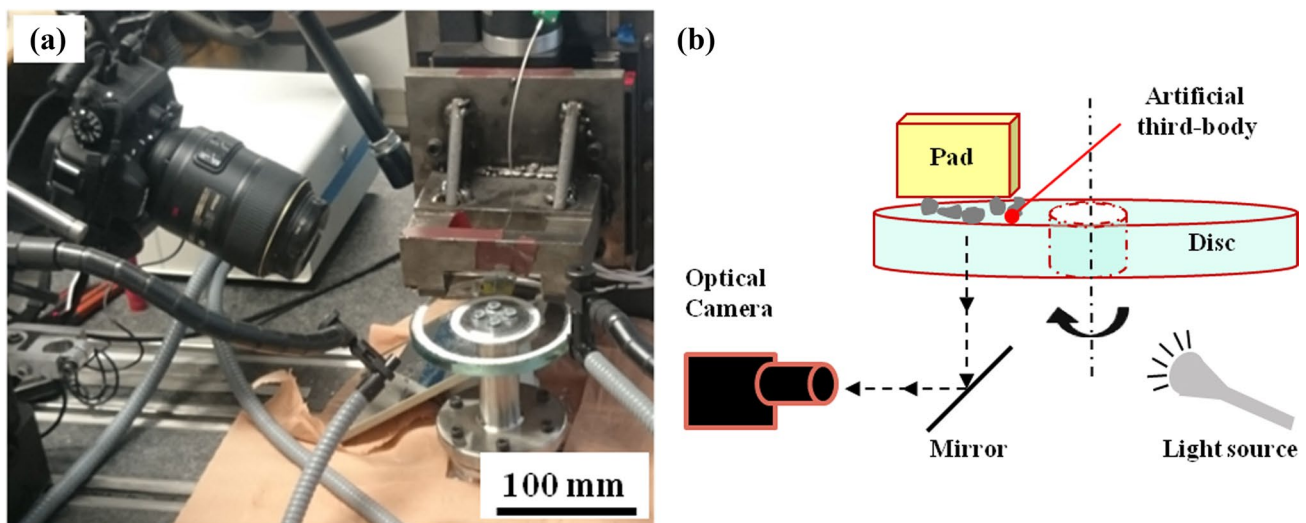


Fig. 3 Set-up instrumentation: **a** general view of instruments used to capture experimental data; **b** schematic illustration of the optical instrumentation

possible for the particles to agglomerate with each other to achieve thick third-body layers.

2.3 Test Procedures

Once the disc and pad are mounted on their respective holders on the test rig (see Fig. 3), some prior adjustments are made such as a correction of disc undulation to limit out-of-plane displacements to a few micrometers. Then, the pad surface is adjusted to be parallel, as much as possible, with respect to the disc. A pressure film is used to assess the disc/pad contact distribution. Before the test is performed (while the disc is stationary) (see illustration in Fig. 4b), adjustments are made by inserting thin spacers between the thin plate and the pad housing. In this study, two kinds of tests were conducted, one without introducing artificial third-body considered as a “reference test,” and the other with the introduction of an artificial third-body called “third-body test”. The “reference test” is necessary to make sure that, without introducing the artificial third-body, there is quasi absence of natural third-body generation coming from the first bodies or any interfacial chemical reaction. Indeed,

natural third-body may interrupt the concept of introducing controlled artificial third-body. Once it is validated that there is no other external factors influencing the system, an artificial third-body has been introduced called “third-body test” which is considered as the key point of the paper. Once the different prior adjustments were made, both the “reference test” and “third-body test” were begun by driving the disc into rotation, without contact with the pad, at a constant angular velocity of 30 rpm. The rotation velocity of 30 rpm was chosen based on several pre-tests to avoid third-body ejection during its deposition on the disc due to centrifugal forces. The test procedures differed between the tests (Reference test and third-body test) while making the contact to take into account the presence of the artificial third-body.

2.3.1 Reference Test

In the reference test, while the disc is rotating, the pad is moved down toward the disc, closing the contact without applying any normal load (zero clearance system position). The system was held in this position for two seconds to make sure that almost zero load is attained. Then, a predefined

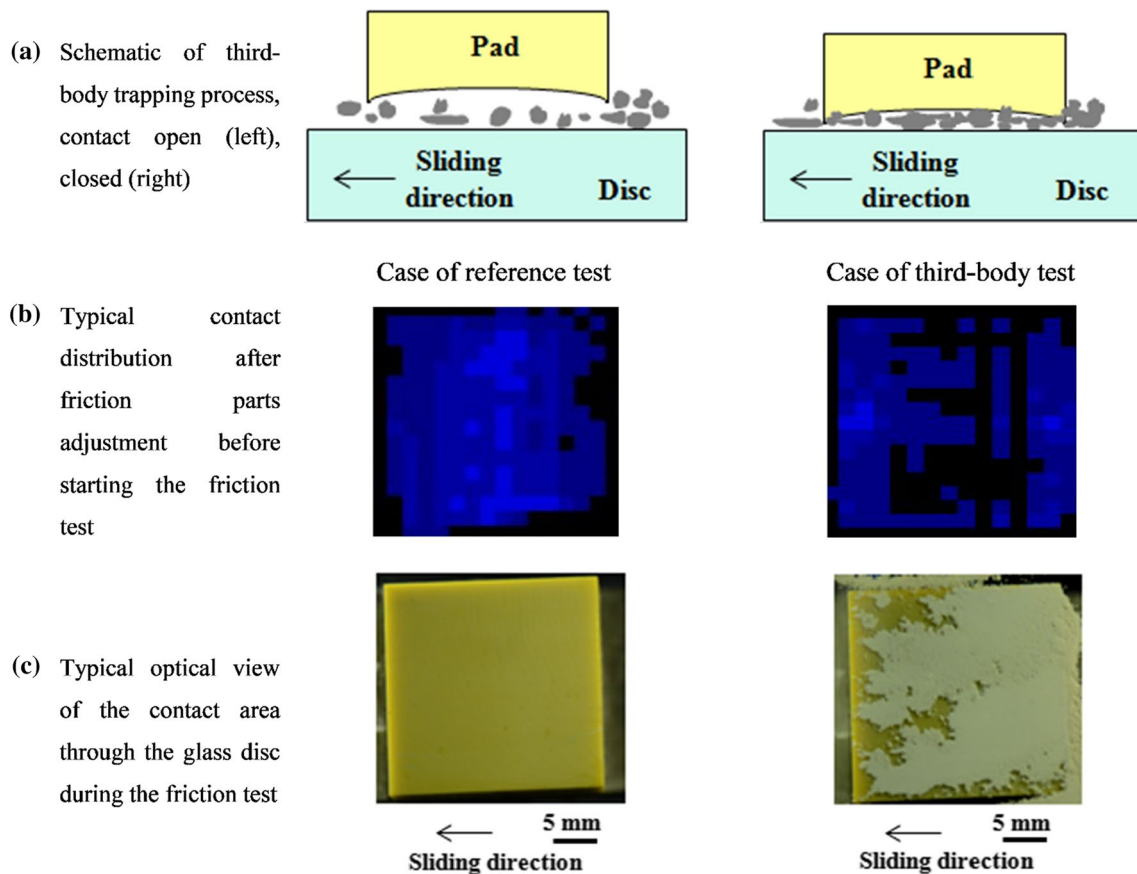


Fig. 4 Test procedure: **a** schematics of capturing the artificial third-body; **b** contact distribution before the experiments (pressure film measurement: low to high pressure from dark to light); **c** optical view of the interface during the experiment

displacement of 40 microns was applied to the extremities of the elastic plate resulting in the application of a normal load of approximately 100 N. Due to out-of-plane displacements induced by the disc undulation, the normal load varies cyclically along with the disc revolutions, depending on the angular position of the disc. The cyclic load variation was close to 3% of the obtained average value for the chosen predefined displacement. The duration of a test was 25 s, and then the test ended by stopping the disc rotation without opening the contact. Figure 4c illustrates the optical view of the disc/pad interface through the transparent disc.

2.3.2 Third-Body Test

In the third-body test, the alumina powder is spread on the rotating disc while the contact is open. Then, the pad is moved down toward the disc to the same zero clearance system position defined for the reference test. It is illustrated in Fig. 4a. The valleys on the pad surface regarding flatness help to trap the third-body between disc/pad interface. As the powder is re-circulating with the disc rotation, more particles are trapped in the interface until the contact is closed. Figure 4b presents the disc/pad contact distribution assessed

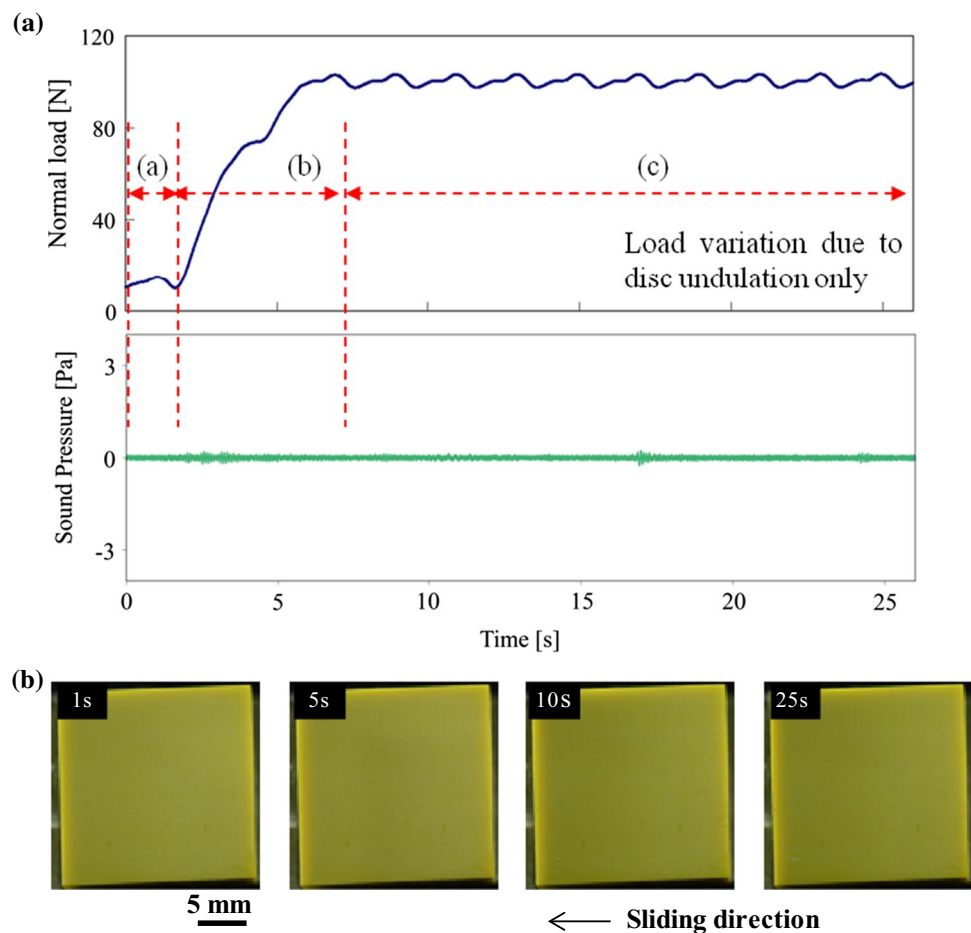
by pressure film before the test. Here, in the figure, the black color represents the pad valleys and zones where there is no disc/pad contact. Figure 4c shows the optical view of trapped third-body in the interface. In this case, due to the presence of the third-body in the pad-disc interface, the thin plate bends earlier, as a consequence of the thickness of the third-body layer, leading to a certain normal loading at 'zero clearance system position' defined above, whereas in the 'Reference test' the pad needed more displacement towards the disc to attain some normal loading. The test lasts for 25 s before being ended by stopping the disc rotation without opening the contact.

3 Results and Discussion

As previously mentioned, two different cases were investigated: (1) without introduction of any artificial third-body (reference test), and (2) with artificial third-body introduction in the interface (third-body test).

Figure 5a shows the time variations of the normal load as well as the sound pressure for the reference test. This typical behaviour can be divided into three successive

Fig. 5 Reference test without introducing artificial third-body: **a** time variation of the normal load and the sound pressure; **b** Optical images of the contact area at different times of the test



stages: (a) first two seconds corresponding to the pad contact with the disc without contact loading (zero clearance system position) (b) from time of 2 s to 7 s corresponding to the increase of the normal load as a result of the increase of the thin plate bending due to additional displacements applied to its extremities towards the disc, and (c) from 7 s until the end of the test, which corresponds to a steady-state of the operational conditions. Stage (c) constitutes indeed the main part of the test in which the variation of the normal load is due to disc undulation only. Regarding sound pressure shown in Fig. 5a, no noise was detected throughout the test, meaning no squeal appears. This quiet and stable behaviour can be correlated to optical observations of the pad–disc interface at different times of the test as shown in Fig. 5b. Indeed, at a macroscopic scale, no change of the contact area can be observed, clearly showing a certain stability of the interface. This silent behaviour has been observed for various testing durations and contact loading conditions, as long as the contact area remains unchanged. On the contrary, the appearance of squeal has been observed, whenever the pad wear occurred.

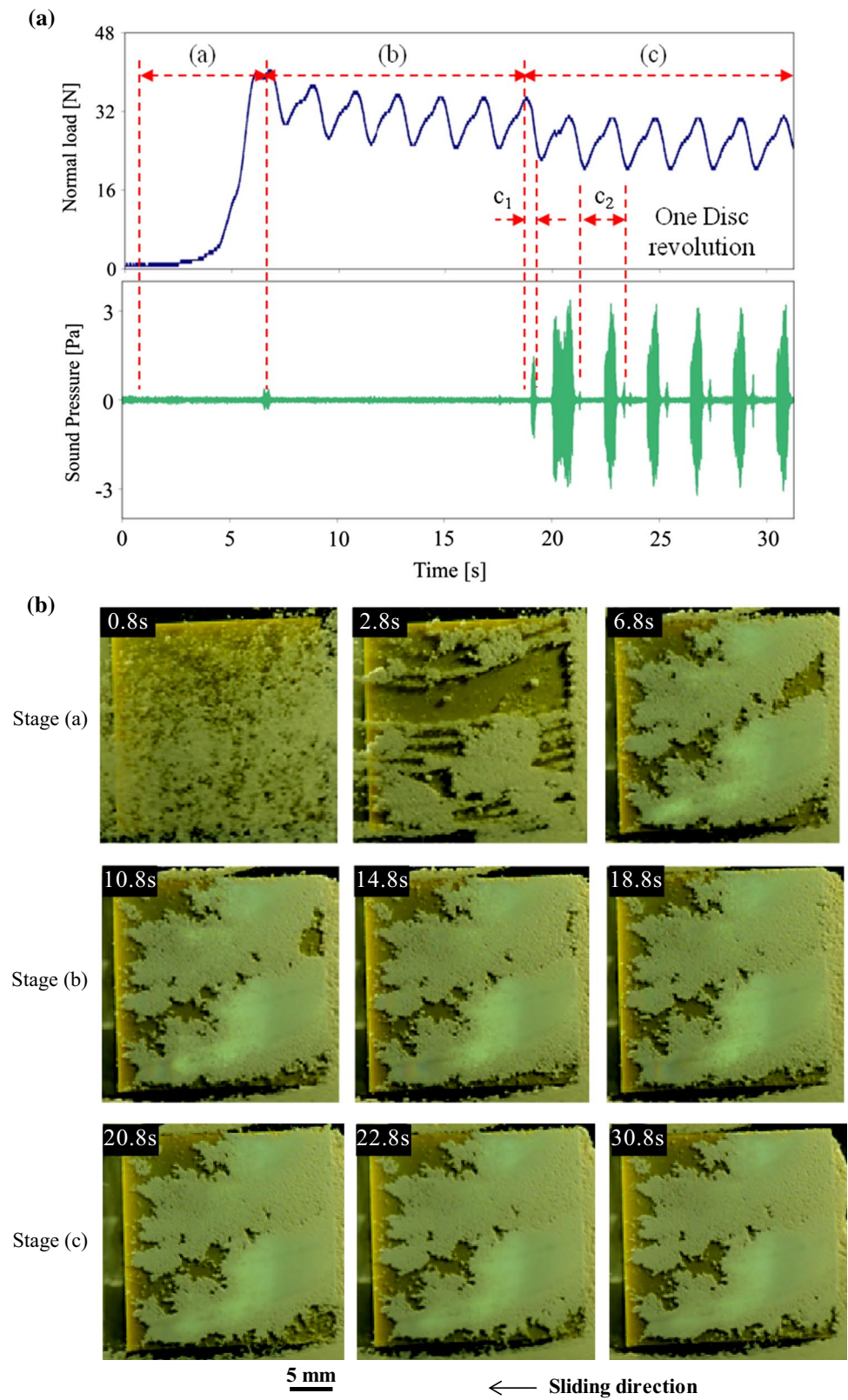
Figure 6a presents the time variation of the normal load and the sound pressure recorded during the third-body test. As mentioned before in Sect. 2.3.2, moving the pad towards the zero clearance system position causes the normal load to increase due to the bending of the thin plate induced by the formation of the artificial third-body layer in the interface. Due to the artificial third-body layer, the first bodies had not any direct contact with each other. The final thickness of the artificial third-body layer was measured after specimen dismounting by an interferometric profilometer and was of the order of 100 μm . The formation of the third-body layer corresponds to the stage (a) in Fig. 6a and can be easily observed with the optical images showing spread, trapping, and compacting of the third-body in the interface as shown in Fig. 6b. It should be clarified that the different optical images presented in Fig. 6b all correspond to the same disc angular position, thus similar contact conditions with respect to the disc undulation. The angular position of the disc corresponds to the maximum normal load. Once zero clearance system displacement is achieved and the third-body layer is trapped in the interface, apart from the disc rotation, no further external intervention is made on the tribological system, and all changes in the contact behaviour arise from the change of the third-body layer and internal flow of alumina particles (redistribution, expand, compaction, etc.). Stage (b) in Fig. 6a corresponds to the steady-state of the operational conditions. The variation of the normal load can be attributed to disc undulation and the stiffness and thickness change of the third-body layer. Two main observations can be made:

- I. A slight progressive decrease in the average normal load can be explained by the cyclic load-loading variation of the third-body layer due to the disc undulation, allowing progressive third-body redistribution by internal flow of alumina particles. It is strongly believed that the redistribution and compaction of the third-body layer decreases its thickness, leading to a reduced normal load.
- II. Absence of noise means that even if the third-body layer and contact conditions progressively change, favorable conditions required for squeal occurrence are still not achieved.

In the following stage (c) (Fig. 6a), three main observations can be made:

- I. A small and brief transitory vibration appears at the beginning of this stage, leading to a sudden drop in the normal load in stage (c₁) (Fig. 6a). This fast reduction in normal force figures out a certain compaction of particles and hence diminution in the third-body layer thickness, as well as changes in the bearing contact zone. The latter can be confirmed by observing the related optical images taken just before and after the transitory vibration (see bright zone corresponding to load-bearing area in Fig. 7). Some fringes can also be seen in Fig. 7, which clearly represent the opening of the contact on the leading side at time 18.9 s and on the trailing side at 19.1 s. This result shows clearly the high capacity of the instrumented experimental set-up to follow and to record fine and fast variations of measured parameters, making it adequate for the study of friction-induced vibrations.
- II. A stabilization of the cyclic normal load variation is obtained after the first brief vibration, meaning that no further notable compaction and/or redistribution of the third-body in the contact occur. This behaviour tends to highlight a certain “dynamic balance” reached between, on one hand, the compaction and redistribution due to disc undulation and, on the other hand the internal third-body flow.
- III. This “quasi-steady-state” is characterized by the periodic occurrence of squeal at the same angular position of the disc. Periodic squeal appears when adequate conditions are fulfilled. These conditions are believed to be related to the compaction ratio of the third-body in the interface (before stage c₂, which is referred to as first full disc revolution in this quasi-steady-state). The compaction of the third-body is apparently one of the key parameters governing the occurrence of squeal in our experimental conditions.

Fig. 6 Third-body test: **a** time variation of the normal load and the sound pressure; **b** time evolution of the third-body layer and contact localization (optical images taken at same angular position of the disc, light reflection—bright zones—corresponds to lead-bearing area localization)



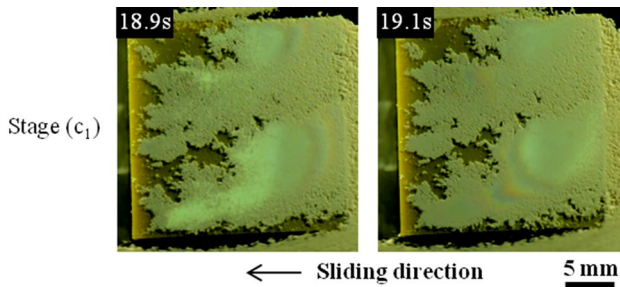


Fig. 7 Optical images of the contact localization, taken just before and after the first small transitory vibration (bright zones—corresponds to load-bearing area localization). The fringes represent the opening of the contact on the leading side at time 18.9 s and on the trailing side at 19.1 s

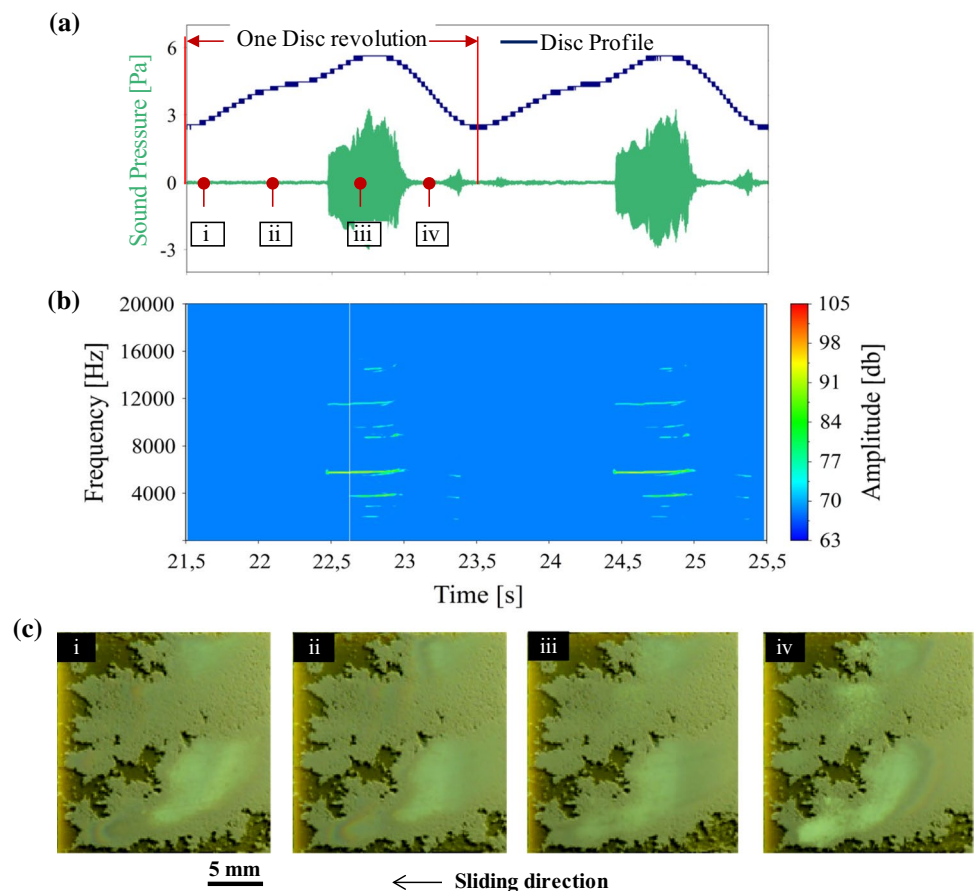
It cannot be excluded that this compaction can influence contact interface stiffness.

It is important to note that during the quasi-steady-state stage, small and very slow changes are believed to occur in contact at very small scales, however, they are undetectable with the used system of optical observation due resolution limits. Preliminary experiments show that prolonging the

experiment in the quasi-steady-state stage leads to the occurrence of another dynamical situation (drastic changes in vibrations, forces, destruction of third-body layers, etc.). In this work, the experiment was intentionally stopped during the quasi-steady-state to conserve the third-body layer for the post-friction measurement of thickness that is 100 μm .

To assess the influence of the disc undulation, a focus has to be made on successive disc revolutions. Figure 8a shows the sound pressure time evolution and the out-of-plane disc displacement for two successive disc revolutions within stage (c) of Figs. 6a and 8b shows a related frequency–time diagram. As can be seen, two main noise events occur periodically at each disc revolution. The frequency as well as the intensity of squeal events are very well reproducible from one cycle to the next, confirming the quasi-steady-state of the tribosystem during this stage of the test. It is important to note that the high intensity squeal event appears when the out-of-plane disc displacement goes up towards a maximum (thus with an increase of the normal load), whereas the low intensity event arises when the out-of-plane disc displacement goes down towards a minimum (thus with a decrease of the normal load). It is clear that the disc undulation causes vibration occurrences. Figure 8c shows the change of the contact localization (in stage c_2 of Fig. 6a) in the

Fig. 8 Quasi-steady-state test stage: **a** cyclic time evolution of sound pressure and out-of-plane disc displacement; **b** related frequency–time diagrams; **c** cyclic change of load-bearing area localization (taken during stage c_2 of Fig. 6a)



friction area along a revolution of the disc. Contact localization oscillates forward and backward vis-à-vis the sliding direction, the disc undulation closing the contact towards the leading edge (from i to iii), while the out-of-plane disc displacement goes up, and towards the trailing edge (from iii to iv) while the out-of-plane disc displacement goes down. This results is in agreement with the dynamical relocation of load-bearing areas during friction suggested in the literature [20]. It can be remarked that this cyclic opening and closure of the contact should affect how third-body particles have degrees of freedom to move or not move inside the third-body layer, i.e., how internal flows of third-body are able to dynamically facilitate the contact accommodation between the first bodies. This last experiment shows a clear correlation of the periodic changes of the friction interface, activated by sliding contact imperfections, with the occurrence of squeal.

4 Conclusions

The experiment assesses the relationship between the change of the third-body layer and the occurrence of squeals in a dry sliding contact. The challenge is to identify contact accommodation mechanisms at a macroscopic scale involving internal flows of third-body particles at a microscopic scale. These mechanisms correspond to the so-called third-body plateaus in the case of real braking systems. To achieve the objective, a specific test rig is used with a transparent disc and a third-body consisting of alumina particles artificially introduced inside the interface. The third-body layer, which completely separates pad and disc, bears the load and continuously accommodates fluctuations of the flat contact due to the relative out-of-plane displacements of moving parts. This accommodation is possible due to the thick artificial third-body layer, made possible by the large size of alumina particles compared to the nano-sized particles of the natural third-body obtained in braking. The time evolution of the contact area is monitored by an optical camera through the transparent glass disc. During testing, no external action is applied to the tribosystem, except for the disc rotation. The loading of the contact is provided by bending the elastic plate in the set-up. Thus, any change of the third-body layer is expected to cause changes in the behaviour of the tribosystem. The following observations were made:

- Whatever the loading or the test duration, as long as the friction interface remains unchanged, the tribosystem initially silent remains silent.
- With an artificial third-body (which acts like natural wear particles in real braking systems), a tribosystem initially silent can become noisy.

- In a noisy tribosystem, the occurrence of squeal is apparently linked to the change in the redistribution of third-body particles in the interface, which strongly influences the location of the load-bearing area.
- The thickness variation and densification of the third-body layer can influence the interface stiffness. The tribosystem is prone to cyclic squealing according to contact closure, alternately towards the leading or the trailing in the sliding direction. This behaviour suggests the existence of a relationship with the inability of the third-body to flow where the load is carried.

Acknowledgements The present research work has been supported by the ELSAT2020 project co-financed by the European Union with the European Regional Development Fund, the French State and the Hauts de France Region Council. The authors gratefully acknowledge the support of these institutions.

References

1. Dufrénoy, P., Bodovillé, G., Degallaix, G.: Damage mechanisms and thermomechanical loading of brake discs. *Eur. Struct. Integr. Soc.* **29**, 167–176 (2002). [https://doi.org/10.1016/S1566-1369\(02\)80073-5](https://doi.org/10.1016/S1566-1369(02)80073-5)
2. Lee, K., Barber, J.R.: An experimental investigation of frictionally-excited thermoelastic instability in automotive disk brakes under a drag brake application. *J. Tribol.* **116**, 409–414 (1994)
3. Österle, W., Dörfel, I., Prietzel, C., Rooch, H., Cristol-Bulthé, A.-L., Degallaix, G., Desplanques, Y.: A comprehensive microscopic study of third body formation at the interface between a brake pad and brake disc during the final stage of a pin-on-disc test. *Wear* **267**, 781–788 (2009). <https://doi.org/10.1016/j.wear.2008.11.023>
4. Kasem, H., Bonnamy, S., Rousseau, B., Estrade-Szwarcckopf, H., Berthier, Y., Jacquemard, P.: Interdependence between wear process, size of detached particles and CO₂ production during carbon/carbon composite friction. *Wear* **263**, 1220–1229 (2007). <https://doi.org/10.1016/j.wear.2007.01.077>
5. Ozcan, S., Filip, P.: Microstructure and wear mechanisms in C/C composites. *Wear* **259**, 642–650 (2005). <https://doi.org/10.1016/j.wear.2005.02.112>
6. Mortelette, L., Brunel, J.F., Boidin, X., Desplanques, Y., Dufrénoy, P., Smeets, L.: Impact of mineral fibres on brake squeal occurrences. SAE International 2009 Brake Colloquium and Exhibition. SAE International, USA (2009). <https://doi.org/10.4271/2009-01-3050>
7. Massi, F., Berthier, Y., Baillet, L.: Contact surface topography and system dynamics of brake squeal. *Wear* **265**, 1784–1792 (2008). <https://doi.org/10.1016/j.wear.2008.04.049>
8. Akay, A.: Acoustics of friction. *J. Acoust. Soc. Am.* **111**, 1525 (2002). <https://doi.org/10.1121/1.1456514>
9. Massi, F., Baillet, L., Giannini, O., Sestieri, A.: Brake squeal: linear and nonlinear numerical approaches. *Mech. Syst. Signal Process.* **21**, 2374–2393 (2007). <https://doi.org/10.1016/j.ymsp.2006.12.008>
10. Kinkaid, N.M., O'Reilly, O.M., Papadopoulos, P.: Automotive disc brake squeal. *J. Sound Vib.* **267**, 105–166 (2003). [https://doi.org/10.1016/S0022-460X\(02\)01573-0](https://doi.org/10.1016/S0022-460X(02)01573-0)

11. Ouyang, H., Nack, W., Yuan, Y., Chen, F.: Numerical analysis of automotive disc brake squeal: a review. *Int. J. Veh. Noise Vib.* **1**, 207–231 (2005). <https://doi.org/10.1504/IJNVN.2005.007524>
12. Giannini, O., Akay, A., Massi, F.: Experimental analysis of brake squeal noise on a laboratory brake setup. *J. Sound Vib.* **292**, 1–20 (2006). <https://doi.org/10.1016/j.jsv.2005.05.032>
13. Conglin, D., Jiliang, M., Chengqing, Y., Xiuqin, B., Tian, Y.: Vibration and noise behaviors during stick—slip friction. *Tribol. Lett.* (2019). <https://doi.org/10.1007/s11249-019-1216-1>
14. Massi, F., Giannini, O., Baillet, L.: Brake squeal as dynamic instability: an experimental investigation. *J. Acoust. Soc. Am.* **120**, 1388–1398 (2006). <https://doi.org/10.1121/1.2228745>
15. Bonnay, K., Magnier, V., Brunel, J.F., Dufrénoy, P., De Saxcé, G.: Influence of geometry imperfections on squeal noise linked to mode lock-in. *Int. J. Solids Struct.* **75–76**, 99–108 (2015). <https://doi.org/10.1016/j.ijsolstr.2015.08.004>
16. Godet, M.: The third-body approach: A mechanical view of wear. *Wear* **100**, 437–452 (1984). [https://doi.org/10.1016/0043-1648\(84\)90025-5](https://doi.org/10.1016/0043-1648(84)90025-5)
17. Berthier, Y.: Maurice Godet's third body. *Tribol. Ser.* **31**, 21–30 (1996). [https://doi.org/10.1016/S0167-8922\(08\)70766-1](https://doi.org/10.1016/S0167-8922(08)70766-1)
18. Jacko, M.G., Tsang, P.H.S., Rhee, S.K.: Wear debris compaction and friction film formation of polymer composites. *Wear* **133**, 23–38 (1989). [https://doi.org/10.1016/0043-1648\(89\)90110-5](https://doi.org/10.1016/0043-1648(89)90110-5)
19. Österle, W., Urban, I.: Friction layers and friction films on PMC brake pads. *Wear* **257**, 215–226 (2004). <https://doi.org/10.1016/j.wear.2003.12.017>
20. Eriksson, M., Lord, J., Jacobson, S.: Wear and contact conditions of brake pads: dynamical in situ studies of pad on glass. *Wear* **249**, 272–278 (2001). [https://doi.org/10.1016/S0043-1648\(01\)00573-7](https://doi.org/10.1016/S0043-1648(01)00573-7)
21. Desplanques, Y., Degallaix, G.: Interactions between third-body flows and localisation phenomena during railway high-energy stop braking. *SAE Int. J. Passeng. Cars Mech. Syst.* **1**, 1267–1275 (2008). <https://doi.org/10.4271/2008-01-2583>
22. Desplanques, Y., Degallaix, G.: Genesis of the third-body at the pad-disc interface: case study of sintered metal matrix composite lining material. *SAE Int. J. Mater. Manf.* **2**, 25–32 (2009). <https://doi.org/10.4271/2009-01-3053>
23. Lee, S., Jang, H.: Effect of plateau distribution on friction instability of brake friction materials. *Wear* **400–401**, 1–9 (2018). <https://doi.org/10.1016/j.wear.2017.12.015>
24. Bergman, F., Eriksson, M., Jacobson, S.: Influence of disc topography on generation of brake squeal. *Wear* **225–229**, 621–628 (1999). [https://doi.org/10.1016/S0043-1648\(99\)00064-2](https://doi.org/10.1016/S0043-1648(99)00064-2)
25. Rhee, S.K., Jacko, M.G., Tsang, P.H.S.: The role of friction film in friction, wear and noise of automotive brakes. *Wear* **146**, 89–97 (1991). [https://doi.org/10.1016/0043-1648\(91\)90226-K](https://doi.org/10.1016/0043-1648(91)90226-K)
26. Hetzler, H., Willner, K.: On the influence of contact tribology on brake squeal. *Tribol. Int.* **46**, 237–246 (2012). <https://doi.org/10.1016/j.triboint.2011.05.019>
27. Magnier, V., Naidoo Ramasami, D., Brunel, J.F., Dufrénoy, P., Chancelier, T.: History effect on squeal with a mesoscopic approach to friction materials. *Tribol. Int.* **115**, 600–607 (2017). <https://doi.org/10.1016/j.triboint.2017.06.031>
28. Richard, D., Iordanoff, I., Renouf, M., Berthier, Y.: Thermal study of the dry sliding contact with third body presence. *J. Tribol.* **130**, 031404 (2008). <https://doi.org/10.1115/1.2913540>
29. Müller, M., Ostermeyer, G.P.: A Cellular Automaton model to describe the three-dimensional friction and wear mechanism of brake systems. *Wear* **263**, 1175–1188 (2007). <https://doi.org/10.1016/j.wear.2006.12.022>
30. Ostermeyer, G.P., Müller, M.: New insights into the tribology of brake systems. *Proc. Inst. Mech. Eng. Part D* **222**, 1167–1200 (2008). <https://doi.org/10.1243/09544070JAUTO595>
31. Österle, W., Orts-gil, G., Gross, T., Deutsch, C., Hinrichs, R., Vasconcellos, M.A.Z.: Impact of high energy ball milling on the nanostructure of magnetite—graphite and magnetite—graphite—molybdenum disulphide blends. *Mater. Charact.* **86**, 28–38 (2013). <https://doi.org/10.1016/j.matchar.2013.09.007>
32. Dmitriev, A. I., Österle, W.: Modelling the sliding behaviour of tribofilms forming during automotive braking: impact of loading parameters and property range of constituents. *Tribol. Lett.* **53**, 337–351 (2013). <https://doi.org/10.1007/s11249-013-0274-z>
33. Magnier, V., Brunel, J.F., Dufrénoy, P.: Impact of contact stiffness heterogeneities on friction-induced vibration. *Int. J. Solids Struct.* **51**, 1662–1669 (2014). <https://doi.org/10.1016/j.ijsolstr.2014.01.005>
34. Kasem, H., Bonnamy, S., Berthier, Y., Jacquemard, P.: Characterization of surface grooves and scratches induced by friction of C/C composites at low and high temperatures. *Tribol. Int.* **43**, 1951–1959 (2010). <https://doi.org/10.1016/j.triboint.2010.03.004>
35. Cristol-Bulthé, A.-L., Desplanques, Y., Degallaix, G.: Coupling between friction physical mechanisms and transient thermal phenomena involved in pad–disc contact during railway braking. *Wear* **263**, 1230–1242 (2007). <https://doi.org/10.1016/j.wear.2006.12.052>
36. Davin, E., Cristol, A., Brunel, J., Desplanques, Y.: Wear mechanisms alteration at braking interface through atmosphere modification. *Wear* **426–427**, 1094–1101 (2019). <https://doi.org/10.1016/j.wear.2019.01.057>
37. Duboc, M., Magnier, V., Brunel, J., Dufrénoy, P., Chancelier, T.: Influence of contact conditions and pad geometry on disc brake squeal noise. In: *European Conference on Braking, JEF2010*. pp. 247–254 (2010)

Publisher's Note Springer Nature remains neutral with regard to jurisdictional claims in published maps and institutional affiliations.